Check for updates

JGR Atmospheres

RESEARCH ARTICLE
10.1029/2020JD033613

Sensitivity of Carbonaceous Aerosol Properties to the Implementation of a Dynamic Aging Parameterization in the Regional Climate Model RegCM

Sudipta Ghosh[1], Nicole Riemer[2], Graziano Giuliani[3], Filippo Giorgi[3], Dilip Ganguly[1], and Sagnik Dey[1]

[1]Center for Atmospheric Sciences, Indian Institute of Technology Delhi, New Delhi, India, [2]Department of Atmospheric Sciences, University of Illinois Urbana-Champaign, Urbana, IL, USA, [3]Earth System Physics Section, The Abdus Salam International Centre for Theoretical Physics, Trieste, Italy

Key Points:

- Hydrophobic black carbon (BC) is converted to hydrophilic BC in <10 h in the polluted Indo-Gangetic Plain as opposed to default 27.6 h in RegCM
- BC concentration increases in the dry season due to the dynamic aging, but reduces in the wet season due to an efficient washout
- Surface dimming increases due to the implementation of the dynamic aging scheme

Supporting Information:

Supporting Information may be found in the online version of this article.

Correspondence to:

S. Dey,
sagnik@cas.iitd.ac.in

Citation:

Ghosh, S., Riemer, N., Giuliani, G., Giorgi, F., Ganguly, D., & Dey, S. (2021). Sensitivity of carbonaceous aerosol properties to the implementation of a dynamic aging parameterization in the regional climate model RegCM. *Journal of Geophysical Research: Atmospheres*, *126*, e2020JD033613. https://doi.org/10.1029/2020JD033613

Received 5 AUG 2020
Accepted 17 AUG 2021

Author Contributions:

Conceptualization: Nicole Riemer, Sagnik Dey
Formal analysis: Sudipta Ghosh
Funding acquisition: Dilip Ganguly, Sagnik Dey
Methodology: Sudipta Ghosh, Nicole Riemer, Graziano Giuliani, Filippo Giorgi, Dilip Ganguly, Sagnik Dey
Project Administration: Dilip Ganguly, Sagnik Dey
Software: Sudipta Ghosh
Supervision: Nicole Riemer, Sagnik Dey
Validation: Sudipta Ghosh
Writing – original draft: Sudipta Ghosh, Sagnik Dey
Writing – review & editing: Nicole Riemer, Graziano Giuliani, Filippo Giorgi, Dilip Ganguly, Sagnik Dey

© 2021. American Geophysical Union. All Rights Reserved.

Abstract Freshly emitted soot is hydrophobic, but condensation of secondary aerosols and coagulation with other particles modify its hygroscopic optical properties. This conversion is referred to as "aerosol aging." Many climate models represent this aging process with a fixed aging time scale, whereas in reality, it is a dynamic process that depends on environmental conditions. Here, we implement a dynamic aging parameterization scheme in the regional climate model RegCM4 in place of the fixed aging timescale of 1.15 days (~27.6 h) and examine its impact on the aerosol life cycle over the Indian subcontinent. The conversion from hydrophobic to hydrophilic aerosol is usually lower than 27.6 h over the entire landmass and lower than 10 h over the polluted Indo-Gangetic Basin (IGB), with seasonal variability. Due to the implementation of the dynamic aging scheme, the column burden and surface mass concentration of carbonaceous aerosols increase during the drier season (December–February) when washout is negligible. The burden is reduced during the wet season (June–September) due to a more efficient washout except over the IGB, where a reduction in precipitation as a result of radiative feedbacks increases the aerosol concentrations. Over the polluted IGB, surface dimming increases due to the dynamic aging scheme, with the top of the atmosphere forcing remaining mostly unchanged. As a result, atmospheric heating increases by at least 1.2 W/m^2. Our results suggest that climate models should incorporate dynamic aging for a more realistic representation of aerosol simulations, especially in highly polluted regions.

Plain Language Summary To understand the impacts of aerosols on air quality and climate, the models need to have a better representation of aerosol processes. One such example is the representation of soot, emitted from fossil-fuel and biomass burning. Many climate models consider soot to be hydrophobic and keep its optical properties constant. However, in reality, this is not true. In this work, we implement the transformation of soot properties in the atmosphere in a regional climate model, RegCM. We found that the soot is converted to hygroscopic in only <10 h in the polluted regions of India relative to a fixed 27.6 h. We discuss the implication of incorporation of such transformation in terms of the changes in aerosol loading, mass concentration, and radiative forcing over the Indian Subcontinent.

1. Introduction

Aerosols continue to be a major source of uncertainty in climate forcing estimates primarily due to the complexity in modeling their life cycles (IPCC, 2013). Carbonaceous aerosols produced as a result of incomplete combustion consists of black carbon (BC) and organic carbon (OC) and contribute a large fraction of the overall aerosol loading, especially in South Asia and India (Bond et al., 2013). BC is emitted directly into the atmosphere from sources, such as vehicles, power plants, industries, and biomass burning. Unlike other aerosol species, BC causes warming at the top of the atmosphere (TOA) and dimming at the surface (Horvath, 1993), and it is considered as a significant potential contributor to global warming (Ramanathan & Carmichael, 2008), with an estimated TOA radiative forcing of 1.1 W/m^2 (Bond et al., 2013).

BC-induced climatic effects play an important role in regulating the Earth's radiation budget at both the global and regional scales (Chung & Seinfeld, 2005; Menon et al., 2002). Hence, a reduction in BC emissions can result in rapid mitigation of global climate warming (Bond et al., 2013; Shindell et al., 2012).

Conversely, OC can be emitted as a primary aerosol from incomplete combustion or formed in the atmosphere by gas-to-particle conversion from volatile organic carbon, that is, in the form of secondary organic carbon (Robinson et al., 2007). Several studies have suggested that OC as a coating can enhance the absorbing property of black carbon by two to four times (Bond et al., 2006; Schnaiter et al., 2005) and also facilitate cloud droplet formation (Yttri et al., 2009).

Southeast Asia, particularly India and China, are important contributors to the global carbonaceous aerosol loading. During the last two decades, several model-based studies have demonstrated the importance of carbonaceous aerosols, and especially BC, in modulating regional climates over various parts of South-East Asia (Bond et al., 2013; Kovilakam & Mahajan, 2016; Lau et al., 2006; Meehl et al., 2008; Menon et al., 2002, and references therein) and over India (Das et al., 2015; Ganguly et al., 2012a; Govardhan et al., 2019; Nair et al., 2012, and the references therein). Carbonaceous aerosols, and in particular BC, influence precipitation over India, leading to an increase of precipitation over the northern regions and a decrease in the south (Chung & Seinfeld, 2005; Menon et al., 2002). BC can also intensify the southwest summer monsoon via an "elevated heat pump" effect over the Indo-Gangetic Plain and Tibetan Plateau (Lau et al., 2006). Meehl et al. (2008) reported that BC could also decrease monsoon rain and increase pre-monsoon precipitation. A similar weakening of the southwest monsoon due to anthropogenic aerosols was reported by Ganguly et al. (2012a) using the CAM global model and Ajay et al. (2019) using the RegCM4 regional model. Das et al. (2015) and Soni et al. (2018) reported that dimming effects by anthropogenic aerosols could induce an anomalous land-sea gradient of temperature, followed by pressure differences which can enhance precipitation over eastern India and the Bay of Bengal.

In spite of being an important climate modulating factor, model estimates of carbonaceous aerosol loading often differ from observations. Various regional studies reported that models are able to capture the BC seasonality (Ajay et al., 2019; Kumar et al., 2015) but underestimate its mass concentration by a factor of 2–5 over the Indian subcontinent (Nair et al., 2012). This underestimation can result from an improper representation of emissions (Ganguly et al., 2012b; Menon et al., 2002; Nair et al., 2012) and/or the inability of the models to accurately represent aerosol processes, such as mixing, aging, removal, and composition (Ganguly et al., 2012a; Govardhan et al., 2019; Meehl et al., 2008; Riemer et al., 2004; Wang et al., 2018). In the recent past, several efforts were aimed at improving emission inventories over the South Asian region (e.g.,Pandey et al., 2014, 2017; Sadavarte & Venkataraman, 2014; Venkataraman et al., 2018), but efforts have been comparatively limited to improve the aerosol life cycle model representation over the region.

Carbonaceous aerosols are hydrophobic when freshly emitted. In the atmosphere, they are converted to hydrophilic particles due to various physical and chemical processes, collectively known as "aging." Neglecting aging can thus lead to biases in the model estimation of the burden of carbonaceous aerosols (Bond et al., 2013; Gustafsson & Ramanathan, 2016). For example, Liu et al. (2016) found that the model estimation of primary carbonaceous aerosols improves across the globe after incorporating microphysical aging in the global model CAM5, particularly over remote regions such as the Arctic. Changes in hygroscopicity due to condensation and coagulation also impact the aerosol optical properties, which in turn affects the radiative forcing of BC (Wang et al., 2018; Wu et al., 2016).

The model implementation of the aging process depends on the model aerosol representation (bulk, sectional or modal, and particle-resolved). Particle-resolved models simulate aerosol aging explicitly and yield a process-level understanding of the aging process (Riemer et al., 2010). On the global scale, models of different complexity have been used to represent the aerosol and their aging processes. Using the sophisticated ATRAS model with a 2D bin structure to represent the BC mixing state, Matsui, Koike, Kondo, Fast, & Takigawa (2014) demonstrate that the BC mixing state is an important parameter for an accurate representation of radiative forcing due to BC absorption. Consideration of aging processes also has a profound impact on the OC burden and formation efficiency (Matsui, Koike, Kondo, Takami, et al., 2014). However, most climate models represent aerosol aging in a highly parameterized way within simplified aerosol modules.

Many models use two tracers for BC (fresh and aged; Chung & Seinfeld, 2002; Cooke et al., 1999) and consider a characteristic e-folding aging time scale to convert "fresh BC" into "aged BC." In the simplest case, this aging time scale is fixed and does not depend on environmental conditions. Croft et al. (2005) compared the fixed aging time scale representation to parameterizations that depend on environmental conditions in

the Canadian general circulation model and concluded that a BC aging treatment that depends on environmental conditions better represents the response of aerosol loadings to future changes in oxidants and pollutants. Similarly, Huang et al. (2012) implemented a variable aging time scale in the GEOS-Chem model, which led to a better simulation of the intercontinental transport of carbonaceous aerosols and lower biases in remote regions of the Northern Hemisphere. They pointed out the importance of chemical aging in polar regions and physical aging in the tropics and midlatitudes.

There are also studies focusing on the influence of carbonaceous aerosol aging on the climate of East Asia. For example, using a novel environmental chamber approach, Peng et al. (2016) demonstrated that the rate and timescale of BC aging are directly proportional to the ambient pollution development and to the aerosol radiative forcing over two cities—Beijing and Houston. Wang et al. (2018) implemented field experiment data to constraint the number of monolayer coatings in the CAM5-MAM4 BC aging scheme and showed that the choice of monolayer coatings could influence both aerosol burden and radiative forcing.

However, to date, no study exists on the importance of aging parameterization in predicting the aerosol loading and optical properties over the Indian sub-continent. Therefore, the focus in this article is on India and the South Asia region. We implement a physical aging parameterization into the regional climate model RegCM4 (Giorgi et al., 2012) to replace the currently used fixed aging time scale of 1.15 days (Cooke et al., 1999). The aging parameterization is a function of aerosol number concentration and condensational flux of secondary aerosol developed by Fierce, Riemer, & Bond (2016) and based on a high-detail particle-resolved modeling approach. Since this full model approach is computationally too expensive to be directly implemented into regional and global climate models (RCMs and GCMs, respectively), Fierce, Bond, et al. (2016) developed several parameterizations of intermediate complexity and computational efficiency to describe dynamic aging (i.e., depending on local environmental conditions). Here, we assess the response of the model to the implementation of the dynamic aging scheme and its climatic effects in a radiatively interactive mode over a domain encompassing South Asia and the Indian sub-continent. In the next section, we present a description of the scheme and its implementation within the RegCM4 framework, followed by a discussion of our results in Section 3.

2. Methodology

2.1. RegCM4 Configuration

We use the regional climate model RegCM4 (Giorgi et al., 2012) developed at the Abdus Salam International Center for Theoretical Physics (ICTP), which has been widely used in various versions for studying the Indian summer monsoon variability, its future evolution, and aerosol-climate interactions over the Indian subcontinent (Das et al., 2015; Dash et al., 2006; Rai et al., 2019; Zhuang et al., 2019). RegCM4 is a hydrostatic, compressible, primitive equation, and sigma-p vertical coordinate model with a dynamical core from the NCAR Mesoscale Model Version 5 (MM5; Grell, 1993). The model can use a wide range of physical parameterizations, and after preliminary test simulations, we selected for our study the Community Climate Model Version 3 (CCM3; Kiehl et al., 1996) radiative transfer scheme with the modifications described in Giorgi et al. (2012), the Biosphere-Atmosphere Transfer Scheme (BATS; Dickinson et al., 1993) for the land surface processes and the University of Washington (UW) scheme (Bretherton et al., 2004; Grenier & Bretherton, 2001; O'Brien et al., 2012) for the planetary boundary layer representation. The Emanuel and Rothman (1999) and Tiedtke (1989) cumulus convection parameterizations are used over land and ocean, respectively, while the SUBEX scheme (Pal et al., 2000) represents large-scale cloud and moisture processes. The model is interactively coupled with both natural (dust and sea salt; Zakey et al., 2006, 2008) and anthropogenic aerosols (Solmon et al., 2006), along with a gas-phase chemistry module (Shalaby et al., 2012).

The anthropogenic aerosols consist of hydrophilic and hydrophobic BC and OC, along with a sulfate scheme described by Qian et al. (2001). The mass concentrations of these species are tracked, assuming that they form an external mixture. The emitted (Figure S1) carbonaceous aerosols are considered to be 80% hydrophobic and 20% hydrophilic for BC, while equal fractions are assumed for hydrophobic and hydrophilic OC. The rate of changes of BC (hydrophobic and hydrophilic BC are indicated by subscript hb and hl) mass mixing ratios are described by the following equations (Solmon et al., 2006):

$$\frac{\partial m^{\text{bc_hb}}}{\partial t} = -\bar{V}.\nabla m^{bc_{hb}} + F_V^{bc_{hb}} + F_H^{bc_{hb}} + T_{\text{CUM}}^{bc_{hb}} + S^{bc_{hb}} - R_{ws,ls}^{bc_{hb}} - R_{ws,\text{cum}}^{bc_{hb}} - \frac{1}{\tau_0} m^{bc_hb}, \quad (1)$$

$$\frac{\partial m^{bc_hl}}{\partial t} = -\bar{V}.\nabla m^{bc_hl} + F_V^{bc_hl} + F_H^{bc_hl} + T_{\text{CUM}}^{bc_{hl}} + S^{bc_hl} - R_{ws,ls}^{bc_hl} - R_{ws,\text{cum}}^{bc_hl} + \frac{1}{\tau_0} m^{bc_hl}, \quad (2)$$

where $-\bar{V}.\nabla m$ = advection, F_V = vertical turbulent diffusion, F_H = horizontal turbulent diffusion, T_{cum} = convective transport which assumes tracers to be well mixed between cloud top and base during convection, S = emission, $R_{w,ls}$ and $R_{w,\text{cum}}$ are the wet removal rates, τ = aging timescale (e-folding time) that quantifies the hydrophobic to hydrophilic conversion. In RegCM4, τ is described by a fixed e-folding time of 1.15 days (Cooke et al., 1999) and $\tau = \tau_0$. The atmospheric lifetime of aerosols is governed by dry and wet deposition. The dry deposition flux varies with the tracer concentration in the lowest level of the model (around 30 m above the surface) and a dry deposition velocity depending on the type of surface. Wet deposition in the RegCM4 is split into "in-cloud" and "below-cloud" terms. The in-cloud removal process occurs in resolvable scale clouds if the cloud liquid water is greater than a threshold level (0.01 g m^{-3}) and is a function of the fractional removal rate of liquid water (fraction of precipitating rain over liquid water content of the atmospheric layer, the in-cloud removal rate for cumulus clouds is constant and fixed at 0.001 s^{-1}) and the aerosol solubility. This solubility is different for different species, and thus hydrophilic, and hydrophobic BC/OC have different in-cloud wet deposition rates. The below-cloud washing out of the aerosols is controlled by their effective diameters and densities. The collection efficiency for each aerosol species is computed from the aerosol effective diameter and density, which is different for different species. In this article, $\tau = \tau_0$ is replaced by $\tau = \tau_{\text{mix}}$ as further explained in Section 2.2.

The model is run over the South-Asian CORDEX domain (20°S–50°N and 10°–130°E) (Giorgi et al., 2009) for a period covering the year 2010 at 0.25° × 0.25° resolution, while the results are analyzed over a focus region covering the Indian subcontinent (0°–45°N and 60°–105°E). The model has 18 vertical levels, with the model top pressure set at 50 hPa. The IIASA emission inventory at a resolution of 0.5° × 0.5° (https://www.iiasa.ac.at/web/home/research/researchPrograms/air/Global_emissions.html) is used for prescribing the sulfate and carbonaceous aerosol emissions for the simulated year (see Figure S1). The initial and lateral meteorological boundary conditions are derived from the ERA-Interim reanalysis data set at 1.5° horizontal resolution and six-hourly temporal resolution, hereafter called EIN15 (Dee et al., 2011). The sea surface temperature is from the NOAA Optimum Interpolated weekly 1° × 1° gridded data. The current RegCM4 version requires chemical boundary conditions, which are derived from the MOZART 6-hourly data. The model is integrated from October 01, 2009, to December 31, 2010, where the first 3 months are considered as spin up and thus are not included in the analysis.

2.2. Parameterization of Carbonaceous Aerosol Aging

Previous studies suggested that the BC aging depends on a number of factors (Riemer et al., 2004, 2010), such as the amount of secondary aerosol that might condense on the BC particles or the underlying aerosol size distribution (Fierce et al., 2015). Fierce, Bond, et al. (2016) used a Monte-Carlo method with the PartMC-MOSAIC model (Riemer et al., 2009; Zaveri et al., 2008) to simulate the evolution of the aerosol through condensation and coagulation. Through a least square regression on the model output, they determined τ_{mix} as a function of condensational growth (I_{cond}) and particle number concentration (N). The time required (τ_{mix}) by freshly emitted particles to become fully mixed is expressed as a function of aerosol number concentration and condensational flux as (Fierce, Bond, et al., 2016):

$$\tau_{\text{mix}} = \frac{1}{I_{\text{cond}} \cdot k_{\text{cond}} + N \cdot k_{\text{coag}}}, \quad (3)$$

where $k_{\text{cond}} = 0.1\ \text{nm}^{-1}$ and $k_{\text{coag}} = 6 \times 10^{-6}\ \text{cm}^3\ \text{h}^{-1}$ (determined from regression). The values for k_{cond} and k_{coag} are calculated separately by applying a least square regression on the model data, considering the effect of condensation and coagulation individually. Here, we implement this scheme in RegCM4 by replacing τ_0 in Equations 1 and 2 with τ_{mix}. Since RegCM4 does not calculate the aerosol number concentration and uses a prescribed characteristic particle radius for the hydrophobic and hydrophilic BC and OC, we diagnose the number concentration for each aerosol tracer (hydrophobic BC, hydrophilic BC, hydrophobic OC,

hydrophilic OC, and sulfate) by assuming a characteristic diameter and then calculate the total number concentration, N, as:

$$N = \sum \frac{M}{D^3 . \rho . \frac{\pi}{6}}, \tag{4}$$

where N = sum of the number concentrations of each tracer, M = mass concentration of a tracer, D = characteristic diameter of a particular tracer (e.g., hydrophobic BC = 0.03 μm, hydrophilic BC = 0.3 μm, hydrophobic OC = 0.2 μm, hydrophilic OC = 0.3 μm, and SO4 = 0.1 μm) and ρ = density of a tracer.

The condensational growth term of Equation 3, I_{cond}, is calculated using the following equation:

$$I_{cond} = \frac{\frac{\partial m_{SO_4}}{\partial t}|_{cond}}{\rho_{SO_4} . S_{aer}}, \tag{5}$$

where $\frac{\partial m_{SO_4}}{\partial t}|_{cond} = SO_4$ condensation mass flux, ρ_{SO4} = density of the sulfate, and S_{aer} = surface area concentration of the aerosol.

2.3. Experimental Design

We carry out two experiments to assess the sensitivity of simulating total anthropogenic aerosols (BC + OC + SO_4) and their climatic effects toward the representation of aerosol aging, one with the new dynamic aging parameterization scheme (hereafter Expt_dyn; Fierce, Bond, et al., 2016) and one with the fixed aging timescale (hereafter Expt_fix; Cooke et al., 1999). Figure 1 shows the mean seasonal anomaly of carbonaceous aerosol aging at the surface (1,000 hPa) with respect to the fixed aging value of 27.6 h (1.15 days), while Figure S2 shows the column average of the aging timescale from 925 to 700 hPa. The Indian climate is divided into four seasons—winter (January–February or JF), pre-monsoon (March–April–May or MAM), monsoon (June–July–August–September or JJAS) and post-monsoon (October–November–December or OND) according to the seasonal classification of the Indian Meteorological Department (http://www.imdpune.gov.in/Weather/Reports/glossary.pdf). Since the aerosol number concentration and condensation flux vary seasonally, the aging timescale also varies seasonally across the domain. Over most of the Indian landmass, the aging time scale is <27.6 h at the surface. Even shorter timescales (<10 h) are observed over the most polluted regions, for example, the IGB, throughout the year. Similarly short aging timescales, ~2 h, were reported by studies over Beijing (Chen et al., 2017; Peng et al., 2016). However, at higher levels above the surface, aging occurs at a slower rate (>27.6 h), except for the winter season (JF). The faster aging rate at the surface can be attributed to the abundance of condensable gases and hygroscopic particles, which enhance the condensation of hydrophilic species and coagulation over these high emission regions. In contrast, large aging timescales (i.e., positive anomaly values) are found across peninsular India, where the anthropogenic sources are limited, and both the number concentration and available condensing particulate matter are comparatively lower. Similar considerations apply to the slower conversion rate found at higher altitudes. Longer aging timescales have also been reported in the literature for locations over central-eastern China (average aging 12 h–7 days) far from the aerosol sources (Chen et al., 2017).

In the next section, we discuss in detail the results for the two contrasting seasons—winter (drier and higher anthropogenic aerosol loading) and monsoon (wetter and lower anthropogenic aerosol loading). Since our focus is the Indian subcontinent, we discuss the changes in aerosol properties within the Indian landmass. Over the oceans, much lower aerosol concentrations are found compared to the landmass since there are hardly any emissions over the oceans (Figure S1). Moreover, from Figure 1, it is evident that the aging time of the carbonaceous aerosols over the oceans is larger than the default aging timescale.

3. Results

We first evaluate the model performance in simulating the meteorological variables (temperature, wind, and precipitation), which play a major role in modulating the life cycle of the carbonaceous aerosols (transport and removal). Next, we examine the changes in aerosol characteristics due to the implementation of the new scheme, followed by a discussion of the changes in aerosol radiative forcing.

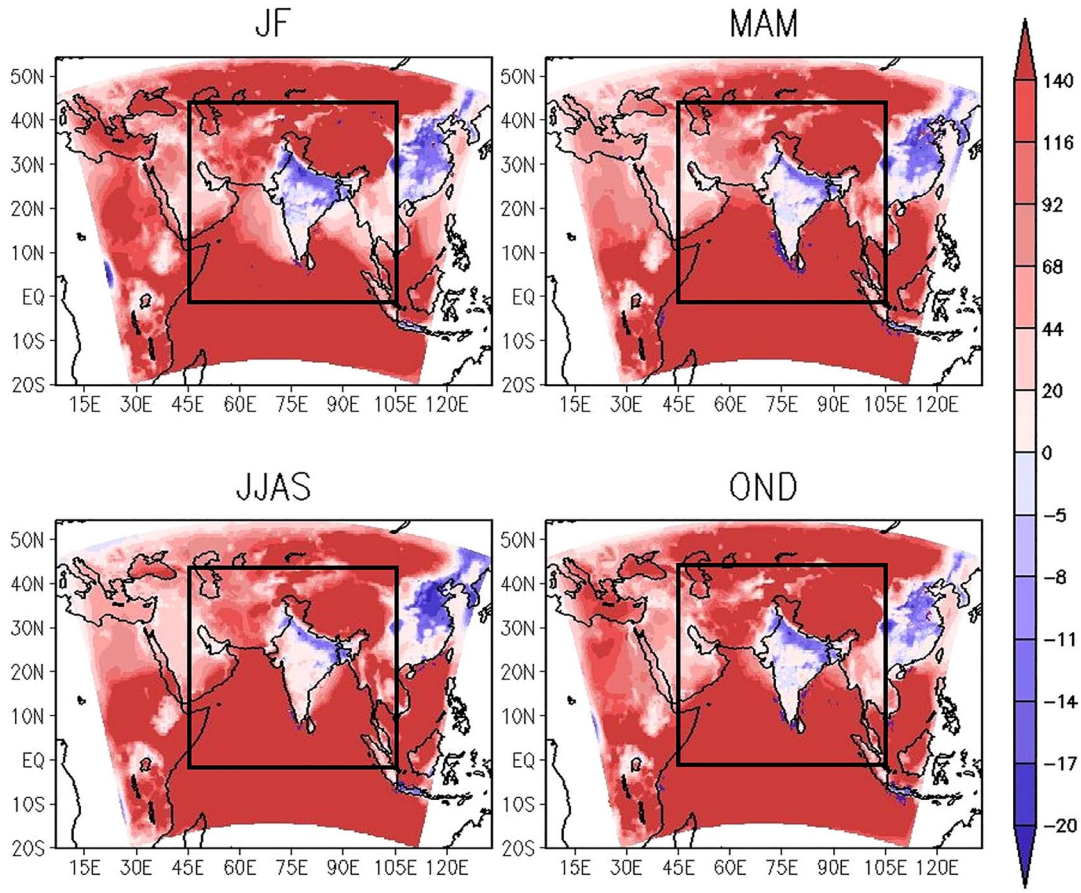

Figure 1. Seasonal variation of aging timescale anomaly (in h) of carbonaceous aerosols at 1,000 hPa w.r.t the fixed aging timescale of 27.6 h (1.15 days). The upper level of the color scale bar has been capped at 140 h (i.e., the aging time scale is [27.6 + 140] h = 167.6 h or 7 days), and the lower limit has been capped at −20 h (i.e., the aging time scale is (27.6−20) h = 7.6 h). The figure shows the complete domain of the simulation, and the area within the black rectangle represents the study domain.

3.1. Model Evaluation

The model captures the seasonal variation of mean near-surface air temperature in both experiments. When compared with CRU data (Figures 2a and 2b), a cold bias of about 3°C is found across parts of the Indian subcontinent in winter, while a better agreement with observations is found over the Himalayan region. During the monsoon (Figures 2c and 2d), a similar bias pattern is observed except over northwest India. Halder et al. (2015) show similar results for the 1983–2005 mean JJAS near-surface temperature simulated by RegCM4. The model is able to capture the seasonal reversal of the wind pattern, that is, north-easterly from land to the ocean during winter (Figure 2e) and south-westerly from ocean to the Indian landmass during the monsoon season (Figure 2g), as reported by earlier studies (Dash et al., 2015; Pattnayak et al., 2018). However, the monsoon flow is somewhat underestimated over the Arabian Sea and overestimated over the Bay of Bengal (Figures 2f and 2h).

The RegCM4 simulated precipitation is compared with Tropical Rainfall Measuring Mission (TRMM) 3-hourly precipitation data available at 0.25° × 0.25° resolution in Figures 2i and 2j. TRMM is a combination of satellite-derived and rain gauge data focusing on the tropical rain band between 50°N and 50°S (Huffman et al., 2007). A dry bias exists over north-western India of ∼8 mm day^{-1}. The agreement between model and observations is fairly good over the central and Deccan plateau region with 0–2 mm day^{-1} bias values. Precipitation is overestimated over north-eastern India and parts of the Bay of Bengal as well as the Arabian Sea. Similar results for precipitation were found over land by Das et al. (2016) and over oceans by Nair et al. (2012). The RMSE values of each meteorological variable are shown in Table 1.

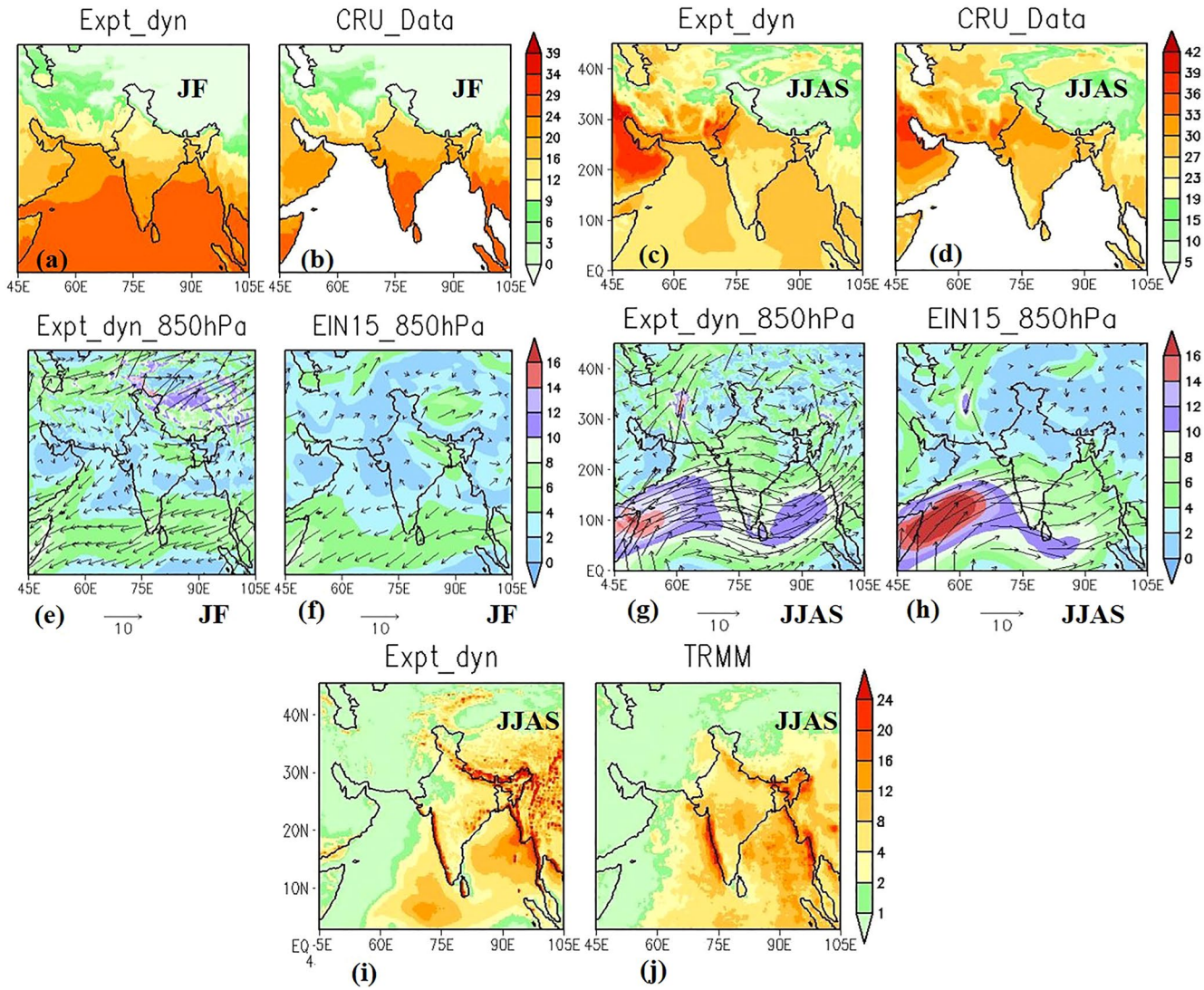

Figure 2. Spatial distribution (a–d) of mean near-surface air temperature (°C), spatial wind pattern (e–h) at 850 hPa (m s^{-1}), and monsoon precipitation (mm day^{-1}) Expt_dyn (i) compared with TRMM data (j).

Thus, our model version simulates the overall spatial distribution of the meteorological parameters essential for aerosol loading in line with previous model experiments, with no significant improvements compared with the standard RegCM4. The main error in the configuration selected appears to be the general cold bias shown in Figures 2a–2d, which may depend on several factors, such as land surface or cloud-related processes.

Table 1
RMSE Values for the Meteorological Fields

	January–February		June–July–August–September	
	Expt_fix	Expt_dyn	Expt_fix	Expt_dyn
Precipitation (mm day^{-1})			5.5	5.6
Temperature (°C)	4.39	4.38	2.89	2.87
Wind_u component (m s^{-1})	2.46	2.47	2.04	1.95
Wind_v component (m s^{-1})	1.89	1.88	2.05	2.00

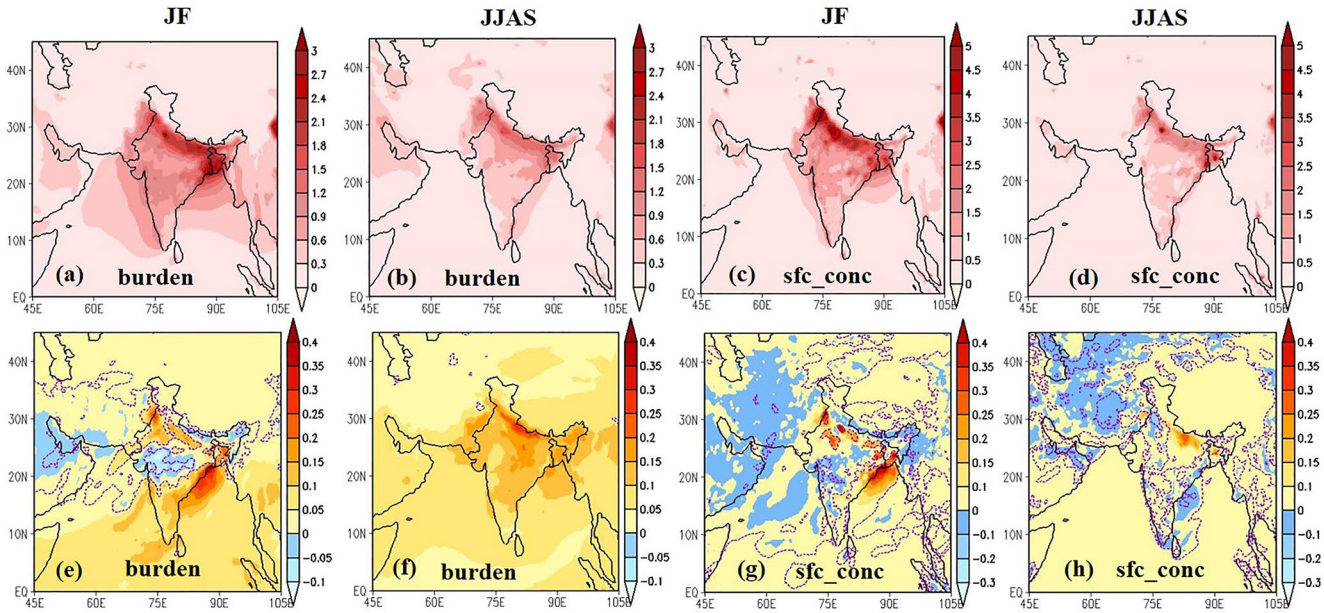

Figure 3. Spatial distribution of mean black carbon (BC) columnar burden (mg m^{-2}) with fixed aging (a and b) and mean BC surface mass concentration (μg m^{-3}) (c and d), corresponding changes due to new aging scheme ([e and f] for columnar burden and [g and h] for surface mass concentration), respectively, for January–February (JF) and June–July–August–September (JJAS) 2010. Dotted lines represent a 75% significance level for burden and an 85% significance level for mass concentration.

3.2. Impact of Dynamic Aging on the Aerosol Spatial Distribution

The horizontal spatial distribution of BC column burden (mg m^{-2}) and surface mass concentration (μg m^{-3}) for the fixed aging scheme are analyzed for the two contrasting seasons, winter (Figures 3a and 3c) and monsoon (Figures 3b and 3d), respectively. High concentrations of BC are observed over the polluted IGB, in agreement with previous studies (Pachauri et al., 2013; Ram & Sarin, 2012; Ram et al., 2010). The column burden is lower over peninsular India compared to the IGB due to lower emissions. The corresponding changes in BC burden and surface concentration due to the implementation of the new aging scheme are shown in Figures 3e and 3g for winter and Figures 3f and 3h for the monsoon season. Positive values imply an increase in concentration when using the dynamic aging scheme.

During winter, the BC column burden increases by almost 6%–7% along with the northern IGB, parts of north-western India, and over the Bay of Bengal when the dynamic aging time scale is used. Increases in BC surface mass concentration show a few hotspots such as Delhi, Punjab, and areas of central Uttar Pradesh, and values of almost 10% over eastern India. A decrease in BC burden is found only over the central-western plains of the Indian sub-continent due to greater dry removal of small hydrophobic particles there (Figure 4e). During the monsoon season, we find prevailing positive changes for surface mass concentration induced by the dynamic aging scheme (at the 85% statistical significance level) throughout most of the Indian sub-continent. Conversely, for the total burden, there is an increase over northern India and a decrease over peninsular India.

These results can be explained as follows. Decreasing the aging time scale in an area will generally result in an accelerated conversion of hydrophobic BC into hydrophilic BC, while increasing the aging time scale results in slower conversion rates (Figure S3). This is then followed by a change in the BC removal rates due to wet and dry deposition. Comparing the relative magnitude of wet and dry deposition fluxes in the model domain, the main removal process of BC is the wet deposition of hydrophilic BC. It may, therefore, seem surprising that we obtain higher BC concentrations in the IGB for the Expt_dyn simulation, where the aging time scale is strongly decreased.

To explain this finding, it is important to note that the spatial distributions of precipitation in simulations Expt_fix and Expt_dyn are different, which in turn impacts wet deposition. In particular, in the Expt_dyn

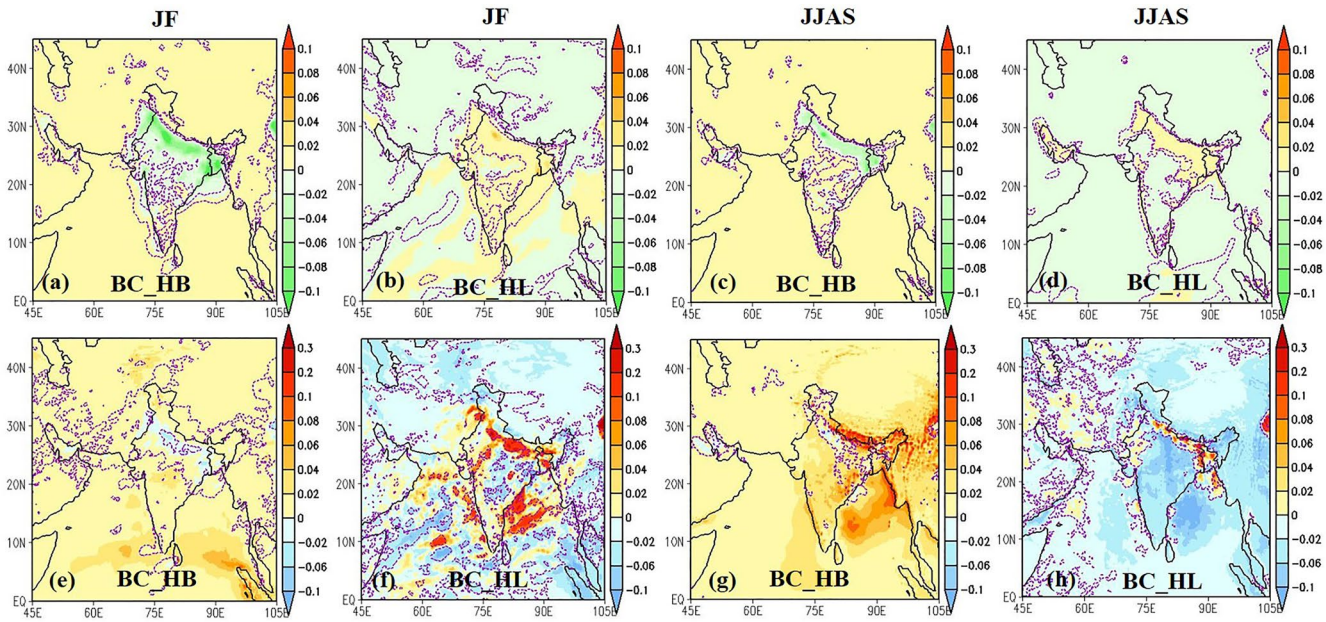

Figure 4. Removal processes for black carbon (BC) (mg m^{-2} day^{-1}): Dry deposition flux difference between Expt_dyn and Expt_fix at 90% significant level for both the seasons (top panel) and wet deposition flux difference values between Expt_dyn and Expt_fix at 90% significant level for DJF and at 80% significant level for June–July–August–September (JJAS) (bottom panel). JF, January–February.

simulation, rainfall during the monsoon season decreases over the IGB and increases in the Himalayan foothills compared to Expt_fix (Figures 7c and 7d). The dynamic timescales are longer than the fixed timescale at higher atmospheric levels where wet removal occurs (Figure S2). Slower conversion to hydrophilic tracer along with reduced rainfall, therefore, contributes to a higher burden in Expt_dyn over some regions.

During winter, the dry season in India, dry deposition becomes relatively more important compared to wet deposition. Also, note that wet and dry deposition interacts in a compensating way, with hydrophilic BC being more prone to wet deposition compared to hydrophobic BC and less prone to dry deposition. This is because the hydrophilic BC tracer is assigned a larger characteristic diameter, which in turn reduces the dry deposition velocity, consistent with the fundamentals of aerosol dynamics (Seinfeld & Pandis, 2016, Ch. 19). The surface concentrations of the hydrophobic and hydrophilic tracers are shown in Figure S4.

These response patterns to the aging scheme are related to delayed and reduced wet removal of hydrophilic particles (Figure 4h) associated with longer aging time scales (Figure 1c). Less efficient wet removal can result in an extended BC lifetime by almost 22.3% (Wang et al., 2018). Over northern India, where aging occurs rapidly (Figure 1c), the hydrophilic wet deposition flux is reduced in Expt_dyn (Figure 4h) due to lower precipitation compared to Expt_fix (Figure 7c), also during the monsoon season. However, wet removal shows a positive increase along the foothills of the Himalayas, where rain also increases. Over peninsular India, aging occurs slowly (Figure 1c), so more hydrophobic particles are available compared to the hydrophilic tracers. Peninsular India receives more rainfall than the rest of India, and therefore wet removal is increased for hydrophobic particles (Figure 4g). In the monsoon season, dry deposition is overcompensated by wet removal.

Changes in OC column burden and surface mass concentration induced by the aging scheme are shown in Figure 5. The increase in column burden (Figure 5e) and surface mass concentration of OC (Figure 5g) have similar spatial patterns as for BC but with greater magnitude and higher significance. The increase in OC burden is primarily tied to biomass burning, which has higher OC content and dominates in the IGB during winter. In particular, the percentage of emitted hydrophilic OC is greater than that of hydrophilic BC, and thus, considering the same aging timescale, this leads to higher OC burdens in the IGB. The OC loading decreases significantly compared to BC over remote regions such as peninsular India during the dry season, and this can be related to low biomass burning in these regions. However, during the monsoon season, the

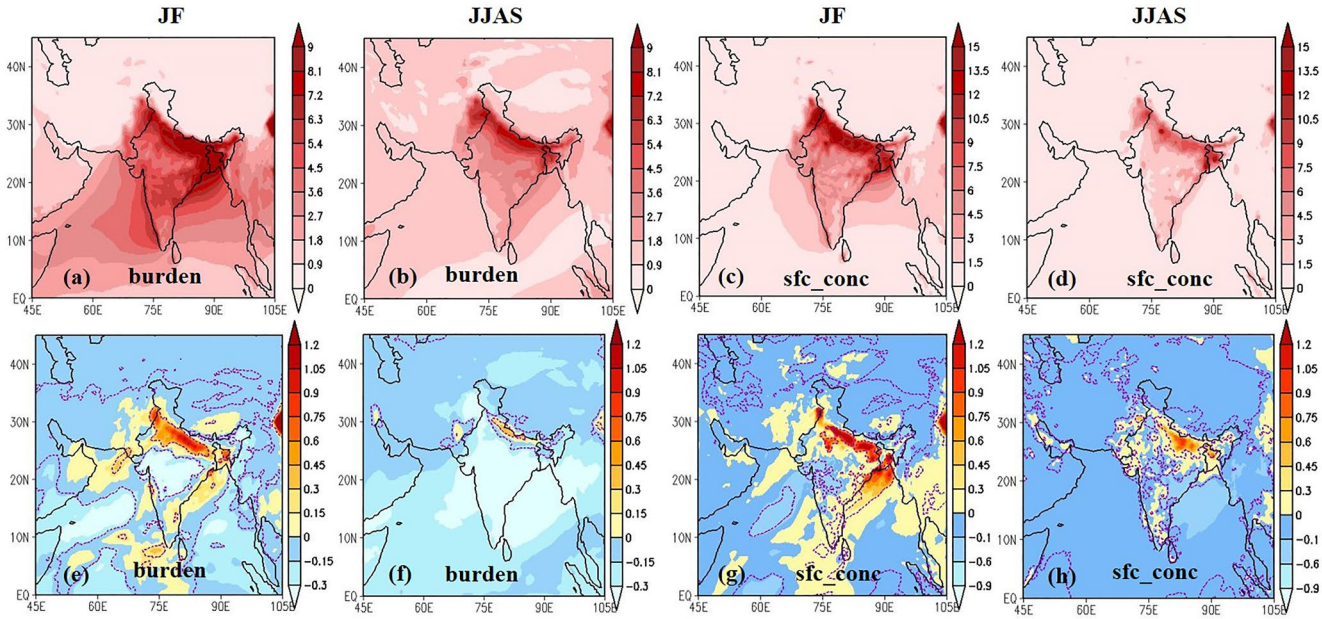

Figure 5. Spatial distribution of mean organic carbon (OC) columnar burden (mg m^{-2}) with fixed aging (a and b) and mean OC surface mass concentration (μg m^{-3}) (c and d), corresponding changes induced due to new aging scheme ([e and f] for columnar burden and [g and h] for surface mass concentration), respectively, for January–February (JF) and June–July–August–September (JJAS) 2010. Dotted lines represent a 75% significance level for burden and an 85% significance level for mass concentration.

OC concentrations show significantly lower values across the entire country compared to the BC concentrations because a higher fraction of OC is scavenged by washout (Huang et al., 2012). A similar result was also found by Ram et al. (2010) for Kanpur and by Priyadharshini et al. (2019) for Kolkata.

Implementation of the dynamic aging scheme induces a BC concentration increase of 0.4% and 5% and an OC concentration increase of 2% and 5.6% in Delhi and Kanpur, respectively. Comparison with in situ observations (values in addition to Delhi and Kanpur are provided in the Table S1) indicates that the simulated BC and OC are still underestimated compared to the observed BC (7.79 ± 3.73 μg m^{-3}) and OC (37.73 ± 14.32 μg m^{-3}) in Delhi (Bisht et al., 2015) and in Kanpur (3.8 ± 2.3 μg m^{-3} for BC and 25.8 ± 16.1 μg m^{-3} for OC; Ram et al., 2010). However, simulated BC surface concentrations (7.15 μg m^{-3} for Delhi and 2.55 μg m^{-3} for Kanpur) fall within the standard deviation of observations, while OC concentrations are highly underestimated (18.69 μg m^{-3} for Delhi and 10.25 μg m^{-3} for Kanpur).

Overall, Table S1 indicates that our model tends to underestimate the carbonaceous aerosol concentrations. There are several potential contributions to this systematic bias, including the simulation of meteorological and aerosol processes and, perhaps more importantly, large uncertainties in emission inventories (Ajay et al., 2019; Nair et al., 2012). As the focus here is to assess the model sensitivity to the aging scheme, assessing these various factors is beyond the scope of this work. However, in order to understand the sensitivity of the combined impact of the aging scheme and higher emissions on the aerosol burden, we perform a sensitivity study by increasing the BC and OC emissions in the dynamic aging experiment by 50% (hereafter Expt_Emissions50).

This sensitivity experiment shows that the aging timescale at 1,000 hPa is faster than the Expt_dyn for both seasons (refer to Figure S5). This lowering of aging timescale in Expt_Emissions50 can be attributed to the availability of a higher concentration of tracers since it is a function of number concentration and condensational flux. When averaged over the Indian sub-continent (7°–38°N and 67°–98°E), the BC concentration is 4.61% higher in winter with dynamic aging relative to the default set-up, but 61.4% higher with the dynamic aging and 50% increased emissions. In the monsoon season, the simulated BC is 5.4% higher than the default set-up with dynamic aging and 58.4% higher with dynamic aging, and 50% increased emissions. This indicates that the model performance is sensitive to both emissions and concentrations but with a

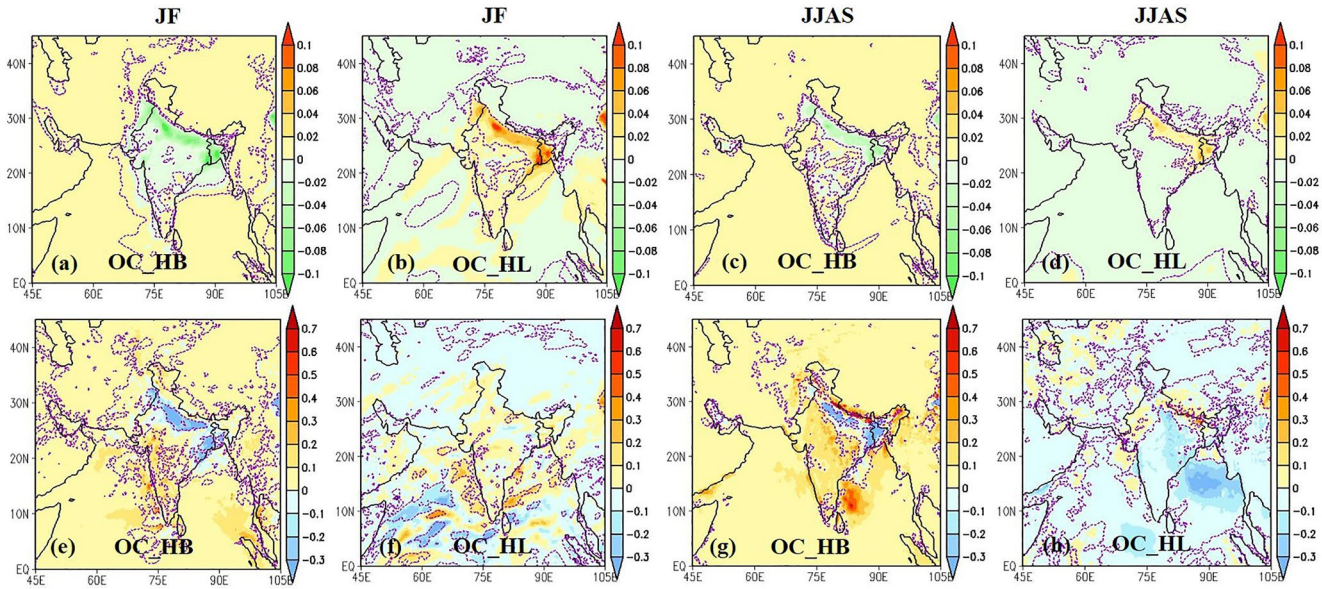

Figure 6. Removal processes for organic carbon (mg m^{-2} day^{-1}): Dry deposition flux difference between Expt_dyn and Expt_fix at 90% significant level for both the seasons (top panel) and wet deposition flux difference values between Expt_dyn and Expt_fix at 90% significance for DJF and at 80% significant level for June–July–August–September (JJAS) (bottom panel). JF, January–February.

higher degree to the emissions. This aspect needs to be further examined using a regionally representative emission inventory.

3.3. Impact of Dynamic Aging on Aerosol Optical Properties

Next, we examine the optical properties of the anthropogenic aerosols and the effect of the new aging scheme. Figures 7a and 7b show the relative changes in anthropogenic AOD induced by the implementation of the dynamical aging scheme for the winter and monsoon seasons, respectively. In Expt_dyn, the mean anthropogenic AOD increases over the IGB (~8%) and decreases over the core monsoon region during winter (Figure 7a), while during the monsoon season (Figure 7b), there is a slight increase (~4%) of AOD over the IGB but a steady decrease over the rest of the country. The change in optical depth during winter can be attributed to the hydrophobic to the hydrophilic ratio of the BC and OC (Figure 8) as well as to the removal processes (Figure 4 for BC and Figure 6 for OC, respectively).

First, an analysis of the ratio of hydrophobic to hydrophilic BC amounts (Figures 8e and 8g for the fixed aging scheme and Figures 8f and 8h for the dynamic aging scheme) shows that the ratio decreases during the winter but remains mostly unchanged during the monsoon season. This effect can be explained as follows. During the dry season, the IGB (the major emission source of India) experiences a peak in emissions due to intense biomass burning. As a result, over the source areas, large amounts of hydrophilic tracers are rapidly generated due to the abundance of coagulating particles and condensing gases. Conversely, the change (from Expt_fix to Expt_dyn) in hydrophobic to the hydrophilic ratio for BC is less pronounced in remote regions (i.e., away from major emitting sources), such as peninsular India. In addition, most of India remains dry during winter; thus, removal by dry deposition (Figures 4 and 6, top panels) plays a dominant role compared to wet removal (Figures 4 and 6, bottom panels). The dry deposition flux of hydrophobic BC (Figure 4a) decreases over the IGB in Expt_dyn due to more hydrophobic to hydrophilic conversion but remains almost unchanged over peninsular India. On the other hand, hydrophilic BC remains unchanged with a 90% significance level over most of India (Figure 4b). This result depends mostly on dry deposition (Seinfeld & Pandis, 2016). As gases condense and particles coagulate on freshly emitted hydrophobic particles, their particle size increases and enters into the size range (0.1–1 μm), where dry deposition velocity decreases with an increase in diameter. Beyond this size range, as the hydrophilic particles grow further,

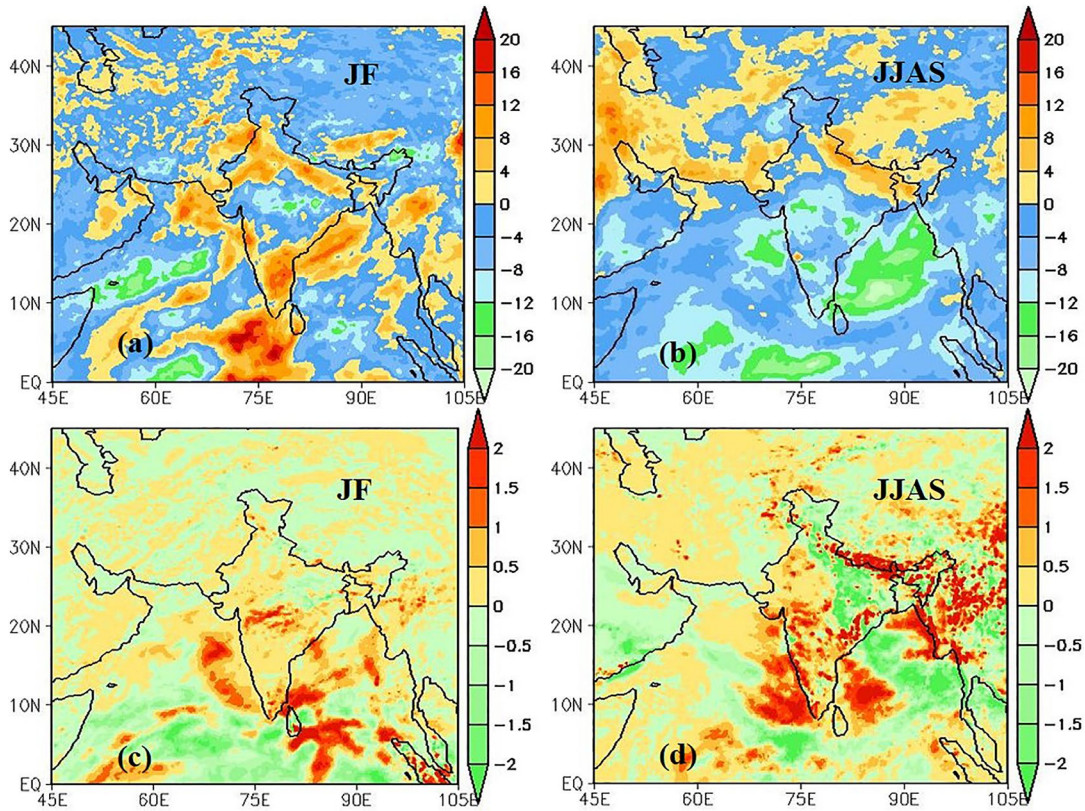

Figure 7. Spatial distribution of % difference of anthropogenic AOD (a and b) and precipitation difference between Expt_dyn and Expt_fix (c and d) for two contrasting seasons.

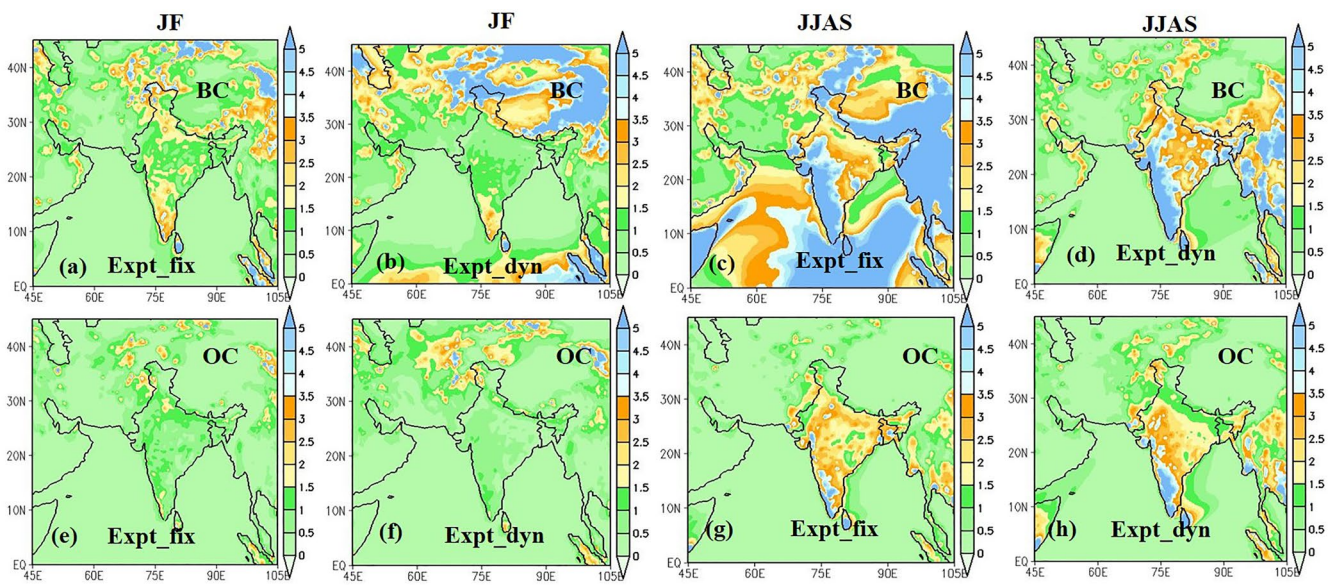

Figure 8. Spatial distributions of black carbon (BC) hydrophobic to the hydrophilic ratio (top panel) and organic carbon (OC) hydrophobic to the hydrophilic ratio (bottom panel) for two contrasting seasons. JF, January–February; JJAS, June–July–August–September.

they are removed by gravity. Matsuda et al. (2012) also reported a dominant role of dry deposition over wet deposition in the removal of carbonaceous aerosols over the tropical forests in Thailand.

During the monsoon season, the ratio of hydrophobic to hydrophilic BC (Figures 8c and 8d) does not show significant changes when changing the aging scheme. The change in dry deposition fluxes of hydrophobic and hydrophilic BC (Figures 4c and 4d) is almost negligible. On the other hand, a positive change in hydrophobic wet removal and a negative change in hydrophilic wet removal produces a counter-balancing effect, which provides a possible explanation for the unchanged hydrophobic to hydrophilic BC ratio.

We then examine the ratio of hydrophobic to hydrophilic OC. During winter (Figures 8e and 8f), this ratio shows a small sensitivity to the aging scheme, likely because the model specifies equal fractions of emitted hydrophilic and hydrophobic OC. Similar to the aging scheme's effect on BC hydrophobic to hydrophilic ratio, dynamic aging results in a reduced OC hydrophobic to hydrophilic ratio over the IGB and an unchanged ratio over peninsular India. Conversely, large effects can be observed during the wet season (Figures 8g and 8h), where faster aging and lower wet removal of hydrophilic tracers over the IGB reduced the ratio, while slower aging along with inefficient wet removal of hydrophobic particles keeps the ratio unaltered over peninsular India.

3.4. Impact of Dynamic Aging on Aerosol Radiative Forcing

Anthropogenic aerosols exert a surface radiative forcing in the range −7 to −10 W m^{-2} in the winter (Figure 9a) and −7 to −9 W m^{-2} in the monsoon season (Figure 9g) over the IGB in Expt_dyn. A similar amount of dimming has been reported in the literature (e.g., Ramanathan & Carmichael, 2008). Over the rest of the Indian landmass, the surface forcing ranges from −3 to −7 W m^{-2}. The spatial pattern of surface forcing closely follows that of the column burdens of BC and OC (Figures 3 and 4). At the TOA, anthropogenic aerosols exert a forcing of −0.005 to −1.5 W m^{-2} over the Indian landmass (Figures 9b and 9h).

Since it is not possible to directly compare the forcing, we compare (Figure 10) the all-sky and clear-sky net surface downward shortwave flux with that from CERES (Doelling et al., 2013; Rutan et al., 2015; Su et al., 2005). Model-derived all-sky and clear-sky fluxes show a similar spatial pattern (e.g., lower flux over the IGB and high-low west-east gradient) as those from CERES. However, the model-derived flux is lower than in CERES. Regression statistics (Figures S6 and S7) show a statistically significant ($p < 0.05$) correlation with the observations for all-sky and clear-sky conditions in JF and for the all-sky conditions in JJAS.

A recent study over China (Zhang et al., 2020) demonstrated that during haze development in polluted conditions, the TOA radiative forcing remains nearly invariant, resulting in little net climatic cooling or warming. Over the desert and snow-covered Himalayan terrain, the TOA forcing switches to a positive sign due to high surface albedo that allows stronger interaction of radiation with aerosols aloft. In the winter, a higher burden of carbonaceous aerosols results in stronger atmospheric heating (Figure 9c) relative to the monsoon season (Figure 9i). Over the polluted IGB and the outflow of the Bay of Bengal, the atmospheric heating is in the range of 9–12 W m^{-2}, while in the monsoon season, it is 4–8 W m^{-2}.

After the implementation of the dynamic aging scheme, during winter, surface dimming (Figures 9a and 9d) increases, and the TOA forcing (Figures 9b and 9e) remains unaltered over the IGB and eastern coasts. For the rest of the country, both surface dimming and TOA forcing do not show significant changes except over central India. A significant TOA forcing in conjunction with unchanged surface dimming over central-eastern India is indicative of BC-rich emissions from power plants and industrial belts located in this region. Decreased surface dimming and unchanged TOA forcing values are observed over central-western India, a remote region from emission sources. As a result of the new aging scheme, the atmospheric heating (Figures 9c and 9f) increases by almost 1.2 W m^{-2} over the IGB. During the monsoon season, although the change in surface dimming is significant over the IGB, the changes at TOA and resulting atmospheric heating are negligible (as it is for the rest of India).

The higher emissions in Expt_Emissions50 result in a higher surface dimming and slightly greater TOA forcing across the sub-continent, which in turn enhances the atmospheric heating by ∼5 W m^{-2}, compared to the default set-up. This result (refer to Figure S8) indicates the probable role of emissions in altering the

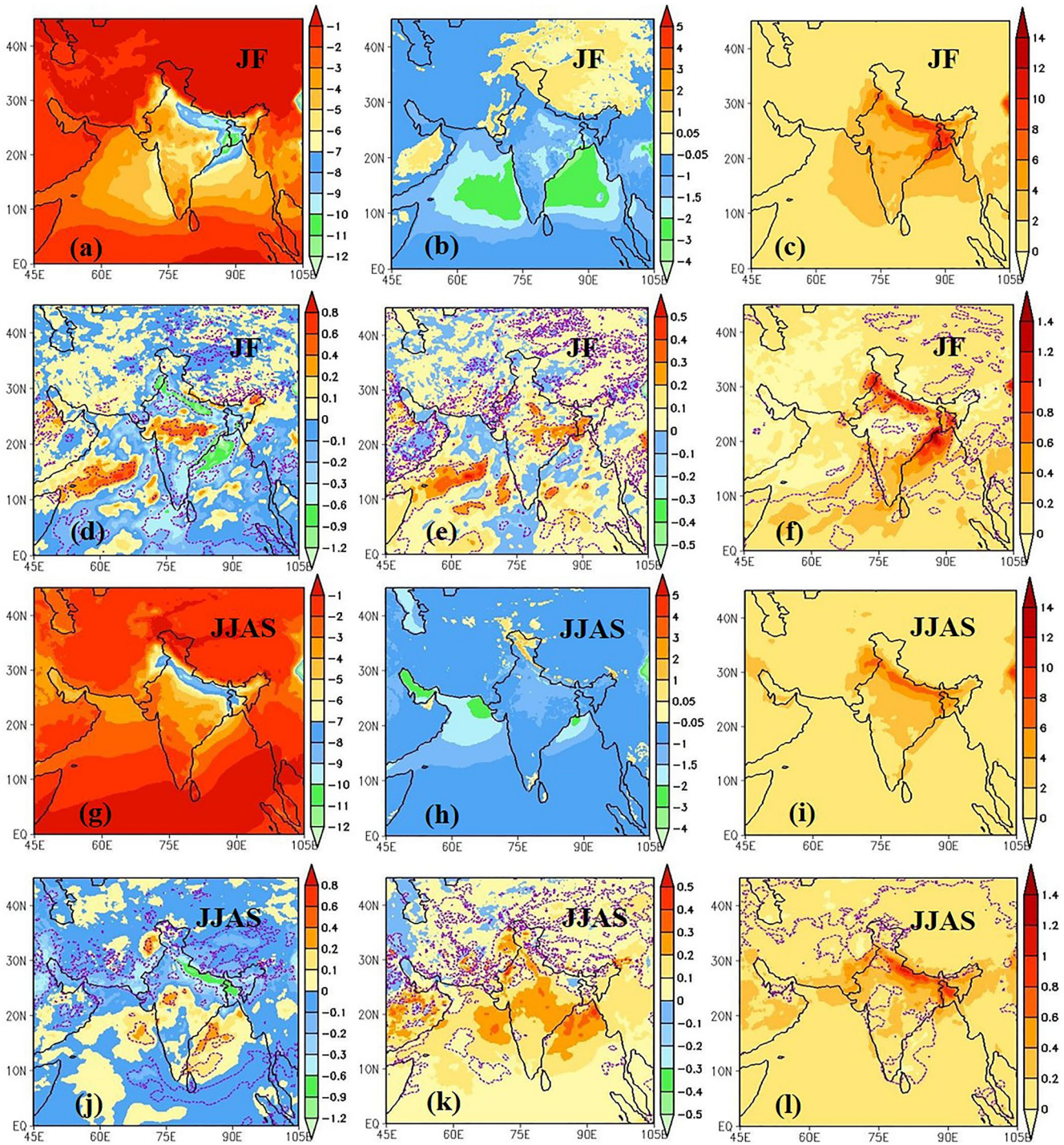

Figure 9. Mean surface shortwave radiative forcing (W m^{-2}) in Expt_dyn and corresponding changes w.r.t Expt_fix for winter (a and d) and monsoon (g and j), mean top of the atmosphere aerosol shortwave forcing (W m^{-2}) in Expt_dyn and corresponding changes w.r.t Expt_fix for winter (b and e) and monsoon (h and k) and mean atmospheric heating (W m^{-2}) in Expt_dyn and corresponding changes w.r.t Expt_fix for winter (c and f) and monsoon (i and l). Dotted contours represent an 85% significance level. JF, January–February; JJAS, June–July–August–September.

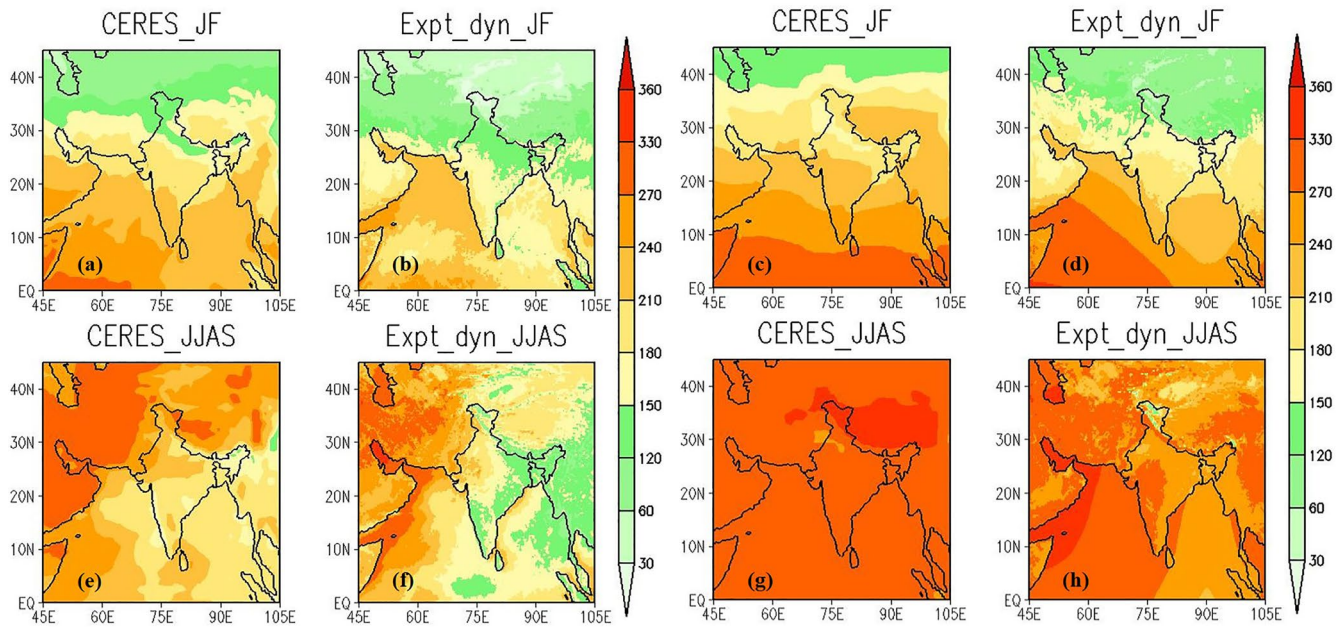

Figure 10. Spatial patterns of seasonal net downward shortwave flux during (a–d) January–February (JF) and (e–h) June–July–August–September (JJAS) in (a, b, e, f) all-sky and (c, d, g, h) clear-sky conditions from (a, c, e, g) CERES and (b, d, f, h) model.

forcing values; however, region-specific emissions would provide a more realistic understanding of this issue.

4. Discussion and Conclusions

Most climate models, if not all, continue to struggle in simulating the observed climate and aerosol characteristics over the Indian monsoon region. The inaccurate representation of aerosol processes is one of the primary factors, and among these processes aging of carbonaceous aerosols is a central one. While, in reality, the BC aging timescale varies depending on the aerosol number concentration and characteristics, most climate models describe this process using a fixed timescale. Here, we implement a dynamic aging parameterization scheme developed by Fierce et al. (2016) in the regional climate model RegCM4 and examine the impact of this implementation on the aerosol column burden and optical properties. Toward this purpose, we examine the sensitivity of the simulated aerosol properties to the implementation of the dynamic aging scheme over a domain covering South Asia.

Key conclusions of our study can be summarized as follows:

1. The implementation of the new aging scheme converts the hydrophobic BC to the hydrophilic BC over polluted regions several hours faster (e.g., smaller than 10 h in the IGB) than the default value of 27.5 h used in the standard version of the model. Conversely, this conversion is slower by several hours than the default value in less polluted regions
2. The ratios of the hydrophobic to the hydrophilic OC and BC change significantly when the dynamic aging scheme is implemented, without a prominent change in the surface concentrations of total carbonaceous aerosols. This suggests the existence of feedback effects on the meteorology, which modify precipitation patterns and, therefore, remove carbonaceous aerosol. Due to a lower hydrophobic to hydrophilic ratio and low values of hydrophilic dry deposition flux, the mean anthropogenic AOD increases by 4%–8% over the IGB and eastern India
3. The atmospheric heating increases by more than 1.2 W m^{-2} in the polluted IGB primarily due to a larger dimming when the dynamic aging scheme is implemented, while TOA forcing remains more or less unchanged

While our results point to the importance of including more detailed representations of aerosol aging in climate/chemistry models, our work can be improved in several directions. First, we use a global emission inventory, which is most likely not very accurate for the Indian region. A regionally specific inventory might thus provide a more detailed description of local emissions and improve the overall agreement of simulated and observed BC and OC concentrations. Second, we limit our simulation time to one year for computing limitations and to assess first-order processes; however, longer simulations would provide more robust assessments of aerosol effects. Third, in our model, we do not include aerosol interactions with clouds, which might be important over the Indian subcontinent, and a parameterization of aerosol indirect effect is only now being implemented in the model. All these aspects are currently being investigated and will be reported in future work.

Data Availability Statement

All data are available from the data portal https://doi.org/10.13012/B2IDB-0533274_V1.

Acknowledgments
This work was supported by the MoEFCC under the NCAP-COALESCE project (Grant No. 14/10/2014-CC). The first author acknowledges the DST-INSPIRE fellowship (IF150055) and the Fulbright-Kalam Climate Doctoral fellowship. Sagnik Dey acknowledges IIT Delhi for Institute Chair. Nicole Riemer acknowledges funding from NSF AGS-1254428 and DOE grant DE-SC0019192. University of Illinois Urbana-Champaign supercomputing facility Keeling and funding from Department of Science and Technology—Funds for Improvement of Science and Technology infrastructure in universities and higher educational institutions (DST-FIST) grant (SR/FST/ESII-016/2014) are acknowledged for the computing support. The authors acknowledge the constructive feedback by the reviewers that helped to improve the manuscript.

References

Ajay, P., Pathak, B., Solmon, F., Bhuyan, P. K., & Giorgi, F. (2019). Obtaining best parameterization scheme of RegCM 4.4 for aerosols and chemistry simulations over the CORDEX South Asia. *Climate Dynamics*, *53*, 329–352. https://doi.org/10.1007/s00382-018-4587-3

Bisht, D. S., Dumka, U. C., Kaskaoutis, D. G., Pipal, A. S., Srivastava, A. K., Soni, V. K., et al. (2015). Carbonaceous aerosols and pollutants over Delhi urban environment: Temporal evolution, source apportionment, and radiative forcing. *Science of the Total Environment*, *521–522*, 431–445. https://doi.org/10.1016/j.scitotenv.2015.03.083

Bond, T. C., Doherty, S. J., Fahey, D. W., Forster, P. M., Berntsen, T., DeAngelo, B. J., et al. (2013). Bounding the role of black carbon in the climate system: A scientific assessment. *Journal of Geophysical Research: Atmospheres*, *118*, 5380–5552. https://doi.org/10.1002/jgrd.50171

Bond, T. C., Habib, G., & Bergstrom, R. W. (2006). Limitations in the enhancement of visible light absorption due to mixing state. *Journal of Geophysical Research*, *111*, D20211. https://doi.org/10.1029/2006jd007315

Bretherton, C. S., McCaa, J. R., & Grenier, H. (2004). A new parameterization for shallow cumulus convection and its application to marine subtropical cloud-topped boundary layers. I. Description and 1D results. *Monthly Weather Review*, *132*, 864–882. https://doi.org/10.1175/1520-0493(2004)132<0864:anpfsc>2.0.co;2

Chen, X., Wang, Z., Yu, F., Pan, X., Li, J., Ge, B., et al. (2017). Estimation of atmospheric aging time of black carbon particles in the polluted atmosphere over central-eastern China using microphysical process analysis in regional chemical transport model. *Atmospheric Environment*, *163*, 44–56. https://doi.org/10.1016/j.atmosenv.2017.05.016

Chung, S. H., & Seinfeld, J. H. (2002). Global distribution and climate forcing of carbonaceous aerosols. *Journal of Geophysical Research*, *107*(D19), 4407. https://doi.org/10.1029/2001jd001397

Chung, S. H., & Seinfeld, J. H. (2005). Climate response of direct radiative forcing of anthropogenic black carbon. *Journal of Geophysical Research*, *110*(D11), 102. https://doi.org/10.1029/2004jd005441

Cooke, W. F., Liousse, C., Cachier, H., & Feichter, J. (1999). Construction of a 1°×1° fossil fuel emission data set for carbonaceous aerosol and implementation and radiative impact in the ECHAM4 model. *Journal of Geophysical Research*, *104*(D18), 22137–22162. https://doi.org/10.1029/1999jd900187

Croft, B., Lohmann, U., & von Salzen, K. (2005). Black carbon ageing in the Canadian Centre for Climate Modelling and Analysis atmospheric general circulation model. *Atmospheric Chemistry and Physics*, *5*, 1931–1949. https://doi.org/10.5194/acp-5-1931-2005

Das, S., Dey, S., & Dash, S. K. (2016). Direct radiative effects of anthropogenic aerosols on Indian summer monsoon circulation. *Theoretical and Applied Climatology*, *124*, 629–639. https://doi.org/10.1007/s00704-015-1444-8

Das, S., Dey, S., Dash, S. K., Giuliani, G., & Solmon, F. (2015). Dust aerosol feedback on the Indian summer monsoon: Sensitivity to absorption property. *Journal of Geophysical Research: Atmospheres*, *120*, 9642–9652. https://doi.org/10.1002/2015jd023589

Dash, S. K., Pattnayak, K. C., Panda, S. K., Vaddi, D., & Mamgain, A. (2015). Impact of domain size on the simulation of Indian summer monsoon in RegCM4 using mixed convection scheme and driven by HadGEM2 Impact of domain size on ISM simulations. *Climate Dynamics*, *44*(3-4). https://doi.org/10.1007/s00382-014-2420-1

Dash, S. K., Shekhar, M. S., & Singh, G. P. (2006). Simulation of Indian summer monsoon circulation and rainfall using RegCM3. *Theoretical and Applied Climatology*, *86*, 161–172. https://doi.org/10.1007/s00704-006-0204-1

Dee, D. P., Uppala, S. M., Simmons, A. J., Berrisford, P., Poli, P., Kobayashi, S., et al. (2011). The ERA-Interim reanalysis: Configuration and performance of the data assimilation system. *Quarterly Journal of the Royal Meteorological Society*, *137*, 553–597. https://doi.org/10.1002/qj.828

Dickinson, R. E., Sellers, H. A., & Kennedy, P. J. (1993). *Biosphere-atmospheretransfer scheme (BATS) version 1E as coupled to the NCAR community climate model* (Technical note NCAR/TN-3871 STR, p. 72). University Corporation for Atmospheric Research. https://doi.org/10.5065/D67W6959

Doelling, D. R., Loeb, N. G., Keyes, D. F., Nordeen, M. L., Morstad, D., Nguyen, C., et al. (2013). Geostationary enhanced temporal interpolation for CERES flux products. *Journal of Atmospheric and Oceanic Technology*, *30*(6), 1072–1090. https://doi.org/10.1175/JTECH-D-12-00136.1

Emanuel, K. A., & Rothman, M. Z. (1999). Development and evaluation of a convection scheme for use in climate models. *Journal of the Atmospheric Sciences*, *56*, 1766–1782. https://doi.org/10.1175/1520-0469(1999)056<1766:daeoac>2.0.co;2

Fierce, L., Bond, T. C., Bauer, S. E., Mena, F., & Riemer, N. (2016). Black carbon absorption at the global scale is affected by particle-scale diversity in composition. *Nature Communications*, *7*, 12361. https://doi.org/10.1038/ncomms12361

Fierce, L., Riemer, N., & Bond, T. (2015). Explaining variance in black carbon's ageing timescale. *Atmospheric Chemistry and Physics*, *15*, 3173–3191. https://doi.org/10.5194/acp-15-3173-2015

Fierce, L., Riemer, N., & Bond, T. (2016). Toward reduced representation of mixing state for simulating aerosol effects on climate. *Bulletin of the American Meteorological Society*, *98*, 971–980.
Ganguly, D., Rasch, P. J., Wang, H., & Yoon, J.-H. (2012a). Climate response of the South Asian monsoon system to anthropogenic aerosols. *Journal of Geophysical Research*, *117*, D13209. https://doi.org/10.1029/2012jd017508
Ganguly, D., Rasch, P. J., Wang, H., & Yoon, J.-H (2012b). Fast and slow responses of the South Asian monsoon system to anthropogenic aerosols. *Geophysical Research Letters*, *39*, L18804. https://doi.org/10.1029/2012gl053043
Giorgi, F., Coppola, E., Solmon, F., Mariotti, L., Sylla, M., Bi, X., et al. (2012). RegCM4: Model description and preliminary tests over multiple CORDEX domains. *Climate Research*, *52*, 7–29. https://doi.org/10.3354/cr01018
Giorgi, F., Jones, C., & Asrar, G. R. (2009). Addressing climate information needs at the regional level: The CORDEX framework. *World Meteorological Organization Bulletin*, *58*(3), 175–183.
Govardhan, G., Satheesh, S. K., Krishna Moorthy, K., & Nanjundiah, R. (2019). Simulations of black carbon over the Indian region: Improvements and implications of diurnality in emissions. *Atmospheric Chemistry and Physics*, *19*, 8229–8241. https://doi.org/10.5194/acp-19-8229-2019
Grell, G. A. (1993). Prognostic evaluation of assumptions used by cumulus parameterizations. *Monthly Weather Review*, *121*, 764–787. https://doi.org/10.1175/1520-0493(1993)121<0764:peoaub>2.0.co;2
Grenier, H., & Bretherton, C. S. (2001). A moist PBL parameterization for large-scale models and its application to subtropical cloudtopped marine boundary layers. *Monthly Weather Review*, *129*, 357–377. https://doi.org/10.1175/1520-0493(2001)129<0357:amppfl>2.0.co;2
Gustafsson, Ö., & Ramanathan, V. (2016). Convergence on climate warming by black carbon aerosols. *Proceedings of the National Academy of Sciences of the United States of America*, *113*(16), 4243–4245. https://doi.org/10.1073/pnas.1603570113
Halder, S., Dirmeyer, P. A., & Saha, S. K. (2015). Sensitivity of the mean and variability of Indian summer monsoon to land surface schemes in RegCM4: Understanding coupled land-atmosphere feedbacks. *Journal of Geophysical Research: Atmospheres*, *120*, 9437–9458. https://doi.org/10.1002/2015JD023101
Horvath, H. (1993). Atmospheric light absorption—A review. *Atmospheric Environment Part A. General Topics*, *27*(3), 293–317. https://doi.org/10.1016/0960-1686(93)90104-7
Huang, Y., Wu, S., Dubey, M. K., & French, N. H. F. (2012). Impact of ageing mechanism on model simulated carbonaceous aerosols. *Atmospheric Chemistry and Physics*, *13*, 6329–6343.
Huffman, G. J., Bolvin, D. T., Nelkin, E. J., Wolff, D. B., Adler, R. F., Gu, G., et al. (2007). The TRMM Multisatellite Precipitation Analysis (TMPA): Quasi-global, multiyear, combined-sensor precipitation estimates at fine scales. *Journal of Hydrometeorology*, *8*(1), 38–55. https://doi.org/10.1175/JHM560.1
IPCC. (2013). *Climate change 2013: The physical science basis. Contribution of working group I to the fifth assessment report of the Intergovernmental Panel on Climate Change*. Intergovernmental Panel on Climate Change.
Kiehl, J. T., Hack, J. J., Bonan, G. B., Boville, B. A., Breigleb, B. P., Williamson, D., & Rasch, P. (1996). *Description of the NCAR community climate model (CCM3)* (Technical report, p. 152). National Center for Atmospheric Research, NCAR/TN-420+STR.
Kovilakam, M., & Mahajan, S. (2016). Confronting the "Indian summer monsoon response to black carbon aerosol" with the uncertainty in its radiative forcing and beyond. *Journal of Geophysical Research: Atmospheres*, *121*, 7833–7852. https://doi.org/10.1002/2016JD024866
Kumar, R., Barth, M. C., Pfister, G. G., Nair, V. S., Ghude, S. D., & Ojha, N. (2015). What controls the seasonal cycle of black carbon aerosols in India? *Journal of Geophysical Research: Atmospheres*, *120*, 7788–7812. https://doi.org/10.1002/2015JD023298
Lau, K. M., Kim, M. K., & Kim, K. M. (2006). Asian summer monsoon anomalies induced by aerosol direct forcing: The role of the Tibetan Plateau. *Climate Dynamics*, *26*(7–8), 855–864. https://doi.org/10.1007/s00382-006-0114-z
Liu, X., Ma, P.-L., Wang, H., Tilmes, S., Singh, B., Easter, R. C., et al. (2016). Description and evaluation of a new four-mode version of the Modal Aerosol Module (MAM4) within version 5.3 of the Community Atmosphere Model. *Geoscientific Model Development*, *9*, 505–522. https://doi.org/10.5194/gmd-9-505-2016
Matsuda, K., Sase, H., Murao, N., Fukazawa, T., Khoomsub, K., Chanonmuang, P., et al. (2012). Dry and wet deposition of elemental carbon on a tropical forest in Thailand. *Atmospheric Environment*, *54*, 282–287. https://doi.org/10.1016/j.atmosenv.2012.02.022
Matsui, H., Koike, M., Kondo, Y., Fast, J. D., & Takigawa, M. (2014). Development of an aerosol microphysical module: Aerosol two-dimensional bin module for formation and ageing simulation (ATRAS). *Atmospheric Chemistry and Physics*, *14*, 10315–10331. https://doi.org/10.5194/acp-14-10315-2014
Matsui, H., Koike, M., Kondo, Y., Takami, A., Fas, J. D., Kanaya, Y., & Takigawa, M. (2014). Volatility basis-set approach simulation of organic aerosol formation in East Asia: Implications for anthropogenic–biogenic interaction and controllable amounts. *Atmospheric Chemistry and Physics*, *14*, 9513–9535. https://doi.org/10.5194/acp-14-9513-2014
Meehl, G. A., Arblaster, J. M., & Collins, W. D. (2008). Effects of black carbon aerosols on the Indian monsoon. *Journal of Climate*, *21*, 2869–2882. https://doi.org/10.1175/2007jcli1777.1
Menon, S., Hansen, J. E., Nazarenko, L., & Luo, Y. (2002). Climate effects of black carbon aerosols in China and India. *Science*, *297*, 2250–2253. https://doi.org/10.1126/science.1075159
Nair, V. S., Solmon, F., Giorgi, F., Mariotti, L., Babu, S. S., & Moorthy, K. K. (2012). Simulation of South Asian aerosols for regional climate studies. *Journal of Geophysical Research*, *117*, D04209. https://doi.org/10.1029/2011jd016711
O'Brien, T. A., Chuang, P. Y., Sloan, L. C., Faloona, I. C., & Rossiter, D. L. (2012). Coupling a new turbulence parametrization to RegCM adds realistic stratocumulus clouds. *Geoscientific Model Development*, *5*, 989–1008. https://doi.org/10.5194/gmd-5-989-2012
Pachauri, T., Satsangi, A., Singla, V., Lakhani, A., & Maharaj Kumari, K. (2013). Characteristics and sources of carbonaceous aerosols in PM2.5 during wintertime in Agra, India. *Aerosol and Air Quality Research*, *13*, 977–991. https://doi.org/10.4209/aaqr.2012.10.0263
Pal, J. S., Small, E. E., & Eltahir, E. A. B. (2000). Simulation of regional-scale water and energy budgets: Representation of subgrid cloud and precipitation processes within RegCM. *Journal of Geophysical Research*, *105*(D24), 29579–29594. https://doi.org/10.1029/2000JD900415
Pandey, A., Patel, S., Pervez, S, Tiwari, S, Yadama, G., Chow, J. C, et al. (2017). Aerosol emissions factors from traditional biomass cookstoves in India: Insights from field measurements. *Atmospheric Chemistry and Physics*, *17*, 13721–13729. https://doi.org/10.5194/acp-17-13721-2017
Pandey, A., Sadavarte, P., Rao, A. B., & Venkataraman, C. (2014). A technology-linked multi-pollutant inventory of Indian energy-use emissions: II. Residential, agricultural and informal industries sectors. *Atmospheric Environment*, *99*, 341–352. https://doi.org/10.1016/j.atmosenv.2014.09.080
Pattnayak, K. C., Panda, S. K., Saraswat, V., & Dash, S. K. (2018). Assessment of two versions of a regional climate model in simulating the Indian Summer Monsoon over South Asia CORDEX domain. *Climate Dynamics*, *50*, 3049–3061. https://doi.org/10.1007/s00382-017-3792-9

Peng, J., Hu, M., Guo, S., Du, Z., Zheng, J., Shang, D., et al. (2016). Markedly enhanced absorption and direct radiative forcing of black carbon under polluted urban environments. *Proceedings of the National Academy of Sciences of the United States of America*, *113*(16), 4266–4271. https://doi.org/10.1073/pnas.1602310113

Priyadharshini, B., Verma, S., Chatterjee, A., Kumar Sharma, S., & Kumar Mandal, T. (2019). Chemical characterization of fine atmospheric particles of water-soluble ions and carbonaceous species in a tropical urban atmosphere over the Eastern Indo-Gangetic Plain. *Aerosol and Air Quality Research*, *19*, 129–147. https://doi.org/10.4209/aaqr.2017.12.0606

Qian, Y., Giorgi, F., Huang, Y., Chameides, W. L., & Luo, C. (2001). Simulation of anthropogenic sulfur over East Asia with a regional coupled chemistry-climate model. *Tellus B*, *53*, 171–191. https://doi.org/10.1034/j.1600-0889.2001.d01-14.x

Rai, P. K., Singh, G. P., & Dash, S. K. (2019). Projected change and variability assessment of Indian summer monsoon precipitation in South Asia CORDEX domain under high-emission pathway. *Pure and Applied Geophysics*, *177*. https://doi.org/10.1007/s00024-019-02373-3

Ram, K., & Sarin, M. M. (2012). Carbonaceous aerosols over Northern India: Sources and spatio-temporal variability. *Proceedings of the Indian National Science Academy*, *78*, 523–533

Ram, K., Sarin, M. M., & Tripathi, S. N. (2010). A 1 year record of carbonaceous aerosols from an urban site in the Indo-Gangetic Plain: Characterization, sources, and temporal variability. *Journal of Geophysical Research*, *115*, D24313. https://doi.org/10.1029/2010jd014188

Ramanathan, V., & Carmichael, G. (2008). Global and regional climate changes due to black carbon. *Nature Geoscience*, *1*, 221–227. https://doi.org/10.1038/ngeo156

Riemer, N., Vogel, H., & Vogel, B. (2004). Soot ageing time scales in polluted regions during day and night. *Atmospheric Chemistry and Physics*, *4*, 1885–1893. https://doi.org/10.5194/acp-4-1885-2004

Riemer, N., West, M., Zaveri, R. A., & Easter, R. C. (2009). Simulating the evolution of soot mixing state with a particle resolved aerosol model. *Journal of Geophysical Research*, *114*, D09202. https://doi.org/10.1029/2008JD011073

Riemer, N., West, M., Zaveri, R. A., & Easter, R. C. (2010). Estimating black carbon ageing timescales with a particle-resolved aerosol model. *Journal of Aerosol Science*, *41*(1), 143–158. https://doi.org/10.1016/j.jaerosci.2009.08.009

Robinson, A. L., Donahue, N. M., Shrivastava, M. K., Weitkamp, E. A., Sage, A. M., Grieshop, A. P., et al. (2007). Rethinking organic aerosols: Semivolatile emissions and photochemical ageing. *Science*, *315*, 1259–1262. https://doi.org/10.1126/science.1133061

Rutan, D. A., Kato, S., Doelling, D. R., Rose, F. G., Nguyen, L. T., Caldwell, T. E., & Loeb, N. G. (2015). CERES synoptic product: Methodology and validation of surface radiant flux. *Journal of Atmospheric and Oceanic Technology*, *32*, 1121–1143. https://doi.org/10.1175/JTECH-D-14-00165.1

Sadavarte, P., & Venkataraman, C. (2014). Trends in multi-pollutant emissions from a technology-linked inventory for India I.Industry and transport sectors. *Atmospheric Environment*, *99*, 353–364. https://doi.org/10.1016/j.atmosenv.2014.09.081

Schnaiter, M., Linke, C., Mohler, O., Naumann, K.-H., Saathoff, H., Wagner, R., et al. (2005). Absorption amplification of black carbon internally mixed with secondary organic aerosol. *Journal of Geophysical Research*, *110*, D19204. https://doi.org/10.1029/2005jd006046

Seinfeld, J. H., & Pandis, S. N. (2016). *Atmospheric chemistry and physics: From air pollution to climate change*.

Shalaby, A., Zakey, A. S., Tawfik, A. B., Solmon, F., Giorgi, F., Stordal, F., et al. (2012). Implementation and evaluation of online gas-phase chemistry within a regional climate model (RegCM-CHEM4). *Geoscientific Model Development*, *5*, 741–760. https://doi.org/10.5194/gmd-5-741-2012

Shindell, D., Kuylenstierna, J. C. I., Vignati, E., Dingenen, R. V., Amann, M., & Klimont, Z., et al. (2012). Simultaneously mitigating near-term climate change and improving human health and food security, *Science*, *335*(6065), 183–189. https://doi.org/10.1126/science.1210026

Solmon, F., Giorgi, F., & Liousse, C. (2006). Aerosol modelling for regional climate studies: Application to anthropogenic particles and evaluation over a European/African domain. *Tellus B: Chemical and Physical Meteorology*, *58*, 51–72. https://doi.org/10.1111/j.1600-0889.2005.00155.x

Soni, P., Tripathi, S. N., & Srivastava, R. (2018). Radiative effects of black carbon aerosols on Indian monsoon: A study using WRF-Chem model. *Theoretical and Applied Climatology*, *132*, 115–134. https://doi.org/10.1007/s00704-017-2057-1

Su, W., Charlock, T. P., & Rose, F. G. (2005). Deriving surface ultraviolet radiation from CERES surface and atmospheric radiation budget: Methodology. *Journal of Geophysical Research*, *110*, D14209. https://doi.org/10.1029/2005JD005794

Tiedtke, M. (1989). A comprehensive mass-flux scheme for cumulus parameterization in large-scale models. *Monthly Weather Review*, *117*, 1779–1800. https://doi.org/10.1175/1520-0493(1989)117<1779:acmfsf>2.0.co;2

Venkataraman, C., Brauer, M., Tibrewal, K., Sadavarte, P., Ma, Q., Cohen, A., et al. (2018). Source influence on emission pathways and ambient PM2.5 pollution over India (2015–2050). *Atmospheric Chemistry and Physics*, *18*, 8017–8039. https://doi.org/10.5194/acp-18-8017-2018

Wang, Y., Ma, P.-L., Peng, J., Zhang, R., Jiang, J. H., Easter, R. C., & Yung, Y. L. (2018). Constraining ageing processes of black carbon in the community atmosphere model using environmental chamber measurements. *Journal of Advances in Modeling Earth Systems*, *10*, 2514–2526. https://doi.org/10.1029/2018ms001387

Wu, Y., Cheng, T., Zheng, L., & Chen, H. (2016). Black carbon radiative forcing at TOA decreased during ageing. *Scientific Reports*, *6*, 38592. https://doi.org/10.1038/srep38592

Yttri, E. K., Myhre, C. L., & Kjetiltørseth (2009). The carbonaceous aerosols—A remaining challenge. *World Meteorological Organization Bulletin*, *58*(1), 54–60.

Zakey, A. S., Giorgi, F., & Bi, X. (2008). Modeling of sea salt in a regional climate model: Fluxes and radiative forcing. *Journal of Geophysical Research*, *113*, D14221. https://doi.org/10.1029/2007JD009209

Zakey, A. S., Solmon, F., & Giorgi, F. (2006). Development and testing of a desert dust module in a regional climate model. *Atmospheric Chemistry and Physics*, *6*, 4687–4704. https://doi.org/10.5194/acp-6-4687-2006

Zaveri, R. A., Easter, R. C., Fast, J. D., & Peters, L. K. (2008). Model for simulating aerosol interactions and chemistry (MOSAIC). *Journal of Geophysical Research*, *113*, D13204. https://doi.org/10.1029/2007JD008782

Zhang, F., Wang, Y., Peng, J., Chen, L., Sun, Y., Duan, L., et al. (2020). An unexpected catalyst dominates formation and radiative forcing of regional haze. *Proceedings of the National Academy of Sciences of the United States of America*, *117*(8), 3960–3966. https://doi.org/10.1073/pnas.1919343117

Zhuang, B. L., Chen, H. M., Li, S., Wang, T. J., Liu, J., Zhang, L. J., et al. (2019). The direct effects of black carbon aerosols from different source sectors in East Asia in summer. *Climate Dynamics*, *53*, 5293–5310. https://doi.org/10.1007/s00382-019-04863-5

References From the Supporting Information

Bisht, D. S., Dumka, U. C., Kaskaoutis, D. G., Pipal, A. S., Srivastava, A. K., Soni, V. K., et al. (2015). Carbonaceous aerosols and pollutants over Delhi urban environment: Temporal evolution, source apportionment, and radiative forcing. *Science of the Total Environment*, *521–522*, 431–445. https://doi.org/10.1016/j.scitotenv.2015.03.083

Chowdhury, Z., Zheng, M., Schauer, J. J., Sheesley, R. J., Salmon, L. G., Cass, G. R., & Russell, A. G. (2007). Speciation of ambient fine organic carbon particles and source apportionment of PM2.5 in Indian cities. *Journal of Geophysical Research*, *112*, D15303. https://doi.org/10.1029/2007JD008386

Gawhane, R. D., Rao, P. S. P., Budhavant, K., Meshram, D. C., & Safai, P. D. (2019). Anthropogenic fine aerosols dominate over the Pune region, Southwest India. *Meteorology and Atmospheric Physics*, *131*, 1497–1508.

Pachauri, T., Singla, V., Satsangi, A., Lakhani, A., & Kumari, K. M. (2013). Characterization of carbonaceous aerosols with special reference to episodic events at Agra, India. *Atmospheric Research*, *128*, 98–110. https://doi.org/10.1016/j.atmosres.2013.03.010

Priyadharshini, B., Verma, S., Chatterjee, A., Kumar Sharma, S., & Kumar Mandal, T. (2019). Chemical characterization of fine atmospheric particles of water-soluble ions and carbonaceous species in a tropical urban atmosphere over the Eastern Indo-Gangetic Plain. *Aerosol and Air Quality Research*, *19*, 129–147. https://doi.org/10.4209/aaqr.2017.12.0606

Ram, K., Sarin, M. M., & Hegde, P. (2008). Atmospheric abundances of primary and secondary carbonaceous species at two high-altitude sites in India: Sources and temporal variability. *Atmospheric Environment*, *42*(28), 6785–6796.

Ram, K., Sarin, M. M., & Tripathi, S. N. (2010). A 1 year record of carbonaceous aerosols from an urban site in the Indo-Gangetic Plain: Characterization, sources, and temporal variability. *Journal of Geophysical Research*, *115*, D24313. https://doi.org/10.1029/2010jd014188

Rengarajan, R., Sarin, M. M., & Sudheer, A. K. (2007). Carbonaceous and inorganic species in atmospheric aerosols during wintertime over urban and high-altitude sites in North India. *Journal of Geophysical Research*, *112*, D21307. https://doi.org/10.1029/2006JD008150

Safai, P. D., Raju, M. P., Budhavant, K. B., Rao, P. S. P., & Devara, P. C. S. (2013). Long term studies on characteristics of black carbon aerosols over a tropical urban station Pune, India. *Atmospheric Research*, *132*, 173–184. https://doi.org/10.1016/j.atmosres.2013.05.002

Satsangi, A., Pachauri, T., Singla, V., Lakhani, A., & Kumari, K. M. (2010). Carbonaceous aerosols at a suburban site in Indo-Gangetic plain. *Indian Journal of Radio and Space Physics*, *39*, 218–222.

Sudheer, A. K., Aslam, M. Y., Upadhyay, M., Rengarajan, R., Bhushan, R., Rathore, J. S., et al. (2016). Kumar, Carbonaceous aerosol over semi-arid region of western India: Heterogeneity in sources and characteristics. *Atmospheric Research*, *178*, 268–278. https://doi.org/10.1016/j.atmosres.2016.03.026